The structure of host-guest complexes between dibenzo-18-crown-6 and water, ammonia, methanol, and acetylene -Evidence of molecular recognition on the complexation-

Ryoji Kusaka, Satoshi Kokubu, Yoshiya Inokuchi, Takeharu Haino,

and Takayuki Ebata*

Department of Chemistry, Graduate School of Science, Hiroshima University,

Higashi-Hiroshima 739-8526, Japan

Abstract

Complexes of dibenzo-18-crown-6 (DB18C6, host) with water, ammonia, methanol, and acetylene (guest), formed in supersonic jets, have been characterized by using various spectroscopic methods: laser induced fluorescence (LIF), UV-UV hole-buning (UV-UV HB), and IR-UV double resonance (IR-UV DR) spectroscopy. Firstly, we reinvestigated the conformations of bare DB18C6 (species **m1** and **m2**) and the structure of DB18C6-H_2O (species **a**) [R. Kusaka, Y. Inokuchi, T. Ebata, *Phys. Chem. Chem. Phys.*, 2008, **10**, 6238] by measuring the IR-UV DR spectra in the region of the methylene CH stretching vibrations. From the IR-UV DR spectra, it was found that the IR spectral feature of the methylene CH stretch of DB18C6-H_2O is clearly different from those of bare DB18C6 conformers, suggesting that DB18C6 changes its conformation when it forms the complex with a water molecule. With the aid of Monte Carlo simulation for extensive conformational search and density functional calculations (at B3LYP and M05-2X/6-31+G* levels), we reassigned the species **m1** and **m2** to the conformers belonging to C_1 and C_2 symmetry, respectively. On the other

hand, we confirmed the DB18C6 part in the species **a** to be "boat" conformation, which is an unstable structure as the bare form. Secondly, we identified nine, one, and two species for DB18C6-ammonia, -methanol, and -acetylene complexes, respectively, by the combination of LIF and UV-UV HB spectroscopy. From the IR-UV DR spectra in the methylene CH stretching region, similar conformational change was identified in the DB18C6-ammonia complex, but not in the complexes with methanol or acetylene. The structures of all the complexes were determined by analyzing the electronic transition energies, exciton splitting, and IR-UV DR spectra in the region of the OH, NH, and CH stretching vibrations. In the DB18C6-ammonia complexes, a NH_3 molecule is incorporated into the cavity of the boat conformation by forming bifurcated and bidentate hydrogen-bond (H-bond), similar to the case of the DB18C6-H_2O complex. On the other hand, in the DB18C6-methanol and -acetylene complexes, methanol and acetylene molecules are simply attached to the C_1 and C_2 conformers, respectively, with their original conformations retained. From the difference of the DB18C6 conformation depending on the type of the guest molecules, it is concluded that DB18C6 distinguishes water and ammonia from methanol and acetylene when it forms complexes, depending on whether guest molecules have an ability to form bidentate H-bonding.

Introduction

Crown ethers (CEs) have been important and fundamental macrocyclic molecules in the host-guest chemistry. They capture variety of guest species, such as metal cations, protonated species and neutral molecules, in their cavity via interactions with multiple oxygen atoms.[1] Applications of CEs, such as phase transfer catalyst[2], photo-switching

devices[3], and drug carriers[4], have been in progress on the basis of the inclusion ability. For characteristic of the encapsulation, it is known that 3*n*-crown-*n* with *n* = 4, 5, and 6 selectively bind Li^+, Na^+ and K^+ alkali ions, respectively, in an aqueous solution[5]. On the other hand, in the gas phase it was reported that 18-crown-6 (18C6) has largest binding energy with Li^+ by folding own flexible conformation[6].

The inclusion ability of CEs is controlled by the delicate balance of the weak interactions among the host, guest, and solvent molecules in addition to the flexible nature of the conformation of CEs. We have been studying structures of CEs and their complexes by using supersonic beam combined with laser spectroscopy[7]. By using the cooling effect of supersonic expansion into vacuum, we can generate weakly bound gaseous complexes with low temperature. The cooling enables us to measure well-resolved electronic and vibrational spectra of the complexes. We have discussed bare conformations of benzo-18-crown-6 (B18C6), dibenzo-18-crown-6 (CB18C6), dibenzo-24-crown-8 (DB24C8), and the structures of their complexes with water or methanol molecules. For B18C6[7(c)], we found that a specific conformer prefers complexation with a water molecule among coexisting several conformers. Similar study has been also carried out by the group of Zwier for benzo-15-crown-5 (B15C5) system, and they found that the B15C5 conformations between bare B15C5 and B15C5-H_2O are different from each other[8].

In the present study, we reinvestigate the conformation of DB18C6 (scheme 1) and the structure of DB18C6-H_2O. In our previous study[7(b)], we identified two bare conformers, species **m1** and **m2**, and assigned that species **m1** to "chair I" form and species **m2** to "boat" form, where **m2** exhibits 5 cm^{-1} exciton splitting. For the DB18C6-H_2O complex, species **a**, we assigned that the DB18C6 part is the boat form

since the complex also exhibits 5 cm^{-1} exciton splitting, similar to the species **m2**. However, the assignment was carried out without studying the CH stretching vibrations, which is sensitive to the conformation of the crown ether frame. So, in order to provide a clear assignment of the conformation of DB18C6, we examine the conformation of bare DB18C6 and DB18C6-H_2O by the IR spectra of the CH stretching vibrations with an aid of quantum chemical calculation. We also discuss whether DB18C6 remains or changes its structure when it forms the complex with a H_2O molecule. We then extend the study to the complexes with various guest molecules: ammonia, methanol, and acetylene. By elucidating the structures of a variety of complexes, we can understand conformational preference of DB18C6 upon each complexation. The study will provide us with the mechanism of the molecular recognition in the host-guest chemistry of crown ethers..

Methods

Experimental: Details of the experiment were described in our previous papers[9]. In brief, we applied laser induced fluorescence (LIF), UV-UV hole-burning (UV-UV HB), and IR-UV double resonance (IR-UV DR) spectroscopy to bare DB18C6 conformers and the DB18C6 complexes with water, ammonia, methanol, and acetylene in supersonic jets. DB18C6 was heated at 120 ºC in the sample housing attached to the commercially available pulsed nozzle (General valve, series 9), and a gaseous mixture of sample/ammonia, methanol, or acetylene vapor diluted with helium buffer gas at a total pressure of 3 atm was expanded into vacuum. The DB18C6-H_2O complex was obtained without adding water vapor because the complex is easily generated with residual water in the sample and gas line. In order to control the partial pressure of

methanol, the temperature of stainless steel bottle containing the liquid was changed by a thermo-regulator. The S_1–S_0 electronic spectra were obtained by LIF spectroscopy and a discrimination of different species was performed by UV-UV HB spectroscopy. The IR spectra of the OH, NH, and CH stretching vibrational region of individual species were obtained by IR-UV DR spectroscopy.

Computational: For a broad conformational exploration, we first carried out Monte Carlo simulation by the mixed torsional search with low-mode sampling [10] in MacroModel V.9.1[11] with MMFF94s force field[12], and optimized the geometries by PRCG algorithm with a convergence threshold of 0.05 kJ/mol. In order to eliminate redundant conformations from the optimized geometries, the maximum distance threshold was set to 1.0 Å and 200 conformers were obtained within 20 kJ/mol energy. All the 200 conformers were optimized by density functional theory (DFT) calculations at B3LYP/6-31+G* level with *loose* optimization criteria using GAUSSIAN 09 program package[13]. The low-lying 10 conformers were re-optimized at the same level with *tight* optimization criteria and *ultrafine* grid, and harmonic IR spectra and electronic transition energies of the re-optimized conformers were calculated. The electronic transition energies were obtained by time-dependent density functional theory (TDDFT) at the same level. In the present study, we also calculated the structure at M05-2X/6-31+G* level, and compared the result with that of B3LYP level. The M05-2X density functional includes van der Waals (vdW) interaction[14], which is thought to be important for estimating the reliable energy of DB18C6 conformers having long oxyethylene chains and two benzene rings. For example, Baek et al. investigated conformers of *L*-Phenylalanine at B3LYP and M05-2X levels[14(d)]. They

reported that both functionals gave the same number of stable conformers, but the relative energies of the conformers predicted by the M05-2X calculation showed better agreement with the observed ones. The M05-2X calculation was also performed for the 200 conformers obtained by the Monte Carlo simulation with the same procedure of the B3LYP calculation. The energies were corrected by non-scaled zero-point vibrational energy. The vibrational frequencies were scaled by the factors of 0.9524 and 0.9270 for B3LYP and M05-2X calculations, respectively. The electronic transition energies obtained by TDDFT method were scaled by the factors of 0.89806 and 0.83576 for B3LYP and M05-2X calculations, respectively.

Results and discussion

1. Bare DB18C6 and DB18C6-H_2O

1.1 IR spectra in the CH stretching region

Figs. 1(a) shows the LIF spectrum of the bare DB18C6 (**m1** and **m2**) and DB18C6-H_2O (species **a**), and Fig. 1(b) displays the IR-UV DR spectra in the CH stretching region of these species. In the IR-UV DR spectra, the bands at 2800-3000 cm^{-1} correspond to the CH stretching vibrations of the methylene groups and those at 3000-3100 cm^{-1} to the CH stretching vibrations of benzene rings. In the methylene CH stretching region, we immediately recognize that the spectral patterns are similar between **m1** and **m2**, while that of the species **a** clearly differs from them. For example, the IR spectra of **m1** and **m2** show a strong band at 2950 cm^{-1}, while the species **a** does not. On the other hand, the IR spectrum of the species **a** shows a strong band at 2830 cm^{-1} and weak one at 2800 cm^{-1}, while such bands are not observed in either **m1** or **m2**. Since the conformation of crown ethers reflects methylene CH stretching vibrations, the

IR spectra indicate that **m1** and **m2** have similar conformation while the DB18C6 conformation of the species **a** is clearly different from them.

To determine the structures of **m1**, **m2** and **a**, we obtained optimized geometries and their IR spectra by DFT calculation. Fig. 2(a) shows five DB18C6 conformers stable at B3LYP or M05-2X levels with the 6-31+G* basis set. The energies (cm^{-1}) relative to the most stable conformer are represented in the parentheses for the two level calculations. For example, conformer I is the most stable at B3LYP, but it is 500 cm^{-1} higher energy than the most stable conformer II at M05-2X. Conformer V was not obtained by B3LYP calculation, so that the relative energy at B3LYP is not shown. Conformer III corresponds to "boat" conformer described in our previous paper[7(c)]. In that paper, we reported that the boat conformer is most stable at B3LYP/6+31G*. However, it turned out that the boat conformer is not the most stable structure. The discrepancy between the previous and present studies is caused by that we did not carry out the initial survey of all the possible conformers by the Monte Carlo simulation in the previous study. On the other hand, in the present study, we performed full survey of possible conformers and could obtain more stable conformers than the boat form. The dihedral angles of each conformer are denoted at the bottom of each column. Other conformers having higher relative energies are shown in Electronic supplementary information (ESI) with their IR and electronic spectra.

Figs. 1(c) and 1(d) show the calculated IR spectra of the optimized structures shown in Fig. 2(a). Fig. 1(e) displays the calculated IR spectra of DB18C6-H_2O shown in Fig. 2(b), in which a water molecule is H-bonded to the boat conformer in the bifurcated and bidentate way. From Figs. 2(c)-(e), we can see that the calculated IR spectra give alost identical patterns for the same structure between B3LYP and M05-2X results,

indicating that the IR spectrum is insensitive to the level of the calculations. In Figs. 2(c) and 2(d), the calculated IR spectra of the boat form (III) are quite different from the other conformers; it has a strong band at 2832 cm^{-1} but no band appears at 2950 cm^{-1}. The calculated IR spectra of the boat conformer are essentially the same with those of boat-H_2O in Fig. 1(e): appearance of the band at 2835 cm^{-1} and no band at 2950 cm^{-1}. Thus, this spectral feature is a characteristic of the boat conformation on IR spectra. By comparing the calculated spectra with the IR-UV DR spectra in Fig. 1(b), we can see that only the calculated IR spectra of the boat form well reproduce IR-UV DR spectrum of the species **a**. In our previous paper, we suggested that the boat-H_2O complex also reproduces the OH stretching vibrations in the IR-UV DR spectrum of the species **a**[7(b)]. Thus, the structure of the species **a** is assigned to the boat-H_2O complex shown in Fig. 2(b). Although the conformations of the species **m1** and **m2** cannot be determined by comparing with calculated IR spectra, their calculated IR spectra strongly suggest that DB18C6 conformations of the species **m1** and **m2** are different from that of the species **a**, that is, conformational change occurs when DB18C6 forms the complex with a H_2O molecule. For more additional structural assignment for the species **m1** and **m2**, we obtained structural information from the electronic spectra of the species **m1** and **m2**.

1.2 Electronic spectra

Fig. 3(a) shows again the LIF spectrum of DB18C6 (species **m1** and **m2**) and DB18C6-H_2O (species **a**). In the LIF spectrum, origin bands of **m1** and **m2** appear at 35597 cm^{-1} and 35688 cm^{-1}, respectively. The position of the electronic transition of DB18C6 sensitively depends on the substituent conformation in the vicinity of the two benzene chromophores. In fact, Zwier group explained S_1-S_0 electronic transition energies of

B15C5 conformers according to their substituent conformation[8]. When four β and γ carbons (see scheme 1) are in the same plane of the benzene ring, the origin of the conformer is located in the 35600-35800 cm^{-1} region. For example, two B15C5 conformers satisfying this condition[8(a)] show their origins at 35645 and 35653 cm^{-1}, and three conformers of B18C6[7(c)] show those at 35628, 35659, and 35666 cm^{-1}. On the other hand, when β or γ carbons are out-of-plane, the electronic transition energies emerge outside of this energy region by several hundred cm^{-1}. For example, the band origin of a conformer with its β carbon out-of-plane appears at 36217 cm^{-1} for B15C5[8(a)], and that of a conformer with its γ carbon out-of-plane appears at 35167 cm^{-1} for B18C6[7(c)]. In case of DB18C6, the band origins of **m1** and **m2** are located at 35600-35800 cm^{-1}, indicating that at least either of the -C_γ-C_β-O(1)-C=C-O(2)-C_β-C_γ- or -C_γ-C_β-O(4)-C=C-O(5)-C_β-C_γ- frames forms the in-plane conformation, where -C=C- represents carbon atoms in a benzene ring.

To find a correlation between the conformation of DB18C6 and the electronic transition energy, we calculated the electronic transition energies by TDDFT for the optimized conformers in Fig. 2. Figs. 3(b) and (c) show the S_1-S_0 and S_2-S_0 transition energies of the bare DB18C6 conformers (red and black stick diagram) and the boat-H_2O complex (blue). The TDDFT results obtained at the B3LYP and M05-2X calculations provide similar electronic transition energies for the same structure, indicating that the TDDFT results are insensitive to the level of the calculations. For the conformer II, both the S_1-S_0 and S_2-S_0 transition energies are located in the region higher than 36000 cm^{-1} because β carbons of each benzene ring are out-of-plane [Fig. 2(a)]. The conformer IV shows the S_1-S_0 transition at 35600 cm^{-1}, and S_2-S_0 transition is located at much higher region because one of four β carbons of the conformer IV is out-of-plane. The conformer V has γ carbons being slightly out-of-plane, so its

transition energies are slightly red-shifted. In the conformers I and III (boat), all the four substituent conformations are in-plane of the corresponding benzene rings nearby, resulting in the S_1-S_0 and S_2-S_0 electronic transitions are located in 35600-35800 cm^{-1} region. Therefore, the DB18C6 conformation reflects the electronic transition energies of the chromophores, and the conformer II can be excluded from the candidate assignable to the species **m1** and **m2** because of its higher electronic transition energies. Since the IR-UV DR spectra in the methylene CH stretching region, as described above, suggest that species **m1** and **m2** are not boat conformer, the candidates assignable to the species **m1** and **m2** are restricted to the conformers I, IV, and V.

In the LIF spectrum of DB18C6 and the DB18C6-H_2O complex [Fig. 3(a)], it should be pointed out that **m1** shows a single origin while **m2** and **a** exhibit a splitting with an interval of 5 cm^{-1}. In our previous paper[7(b)], we concluded that the splitting is ascribed to the exciton splitting, and the single peak of the species **m1** is due to symmetry restriction of this conformer. Since the exciton splitting occurs when the electronic transitions of the two chromophores are degenerated, two chromophores should be located in the same or very similar environment, so the species **m2** is assignable to either of conformers I or V [Fig. 2(a)]. The splitting between the S_1-S_0 and S_2-S_0 electronic transitions is 74 and 167 cm^{-1} at M05-2X level for conformers I and V, respectively [Fig. 3(c)]. The actual splitting is obtained by taking into account the Franck-Condon part of the electronic transitions[7(b)]. The obtained exciton splitting is 7.4 and 16.7 cm^{-1} for conformer I and V, respectively. Since the value of the conformer I (7.4 cm^{-1}) is in good agreement with the observed one (5 cm^{-1}), the species **m2** can be assignable to the conformer I.

For the species **m1**, we assigned it to “chair I” conformer which has C_i symmetry in

our previous paper[7(b)] due to its inversion symmetry. However, the chair I conformer is found to be a high energy conformer: 831 and 1230 cm^{-1} at B3LYP and M05-2X levels, respectively. So, the appearance of the single band peak will be attributed to another reason. Another possibility is that the conformations near benzene chromophores are different between two benzene rings. This is the case of conformer IV which has C_1 symmetry [Fig. 2(a)], and it shows largely separated S_1-S_0 and S_2-S_0 transitions [Fig. 3(a) and 3(c)], resulting in a single peak of the S_1-S_0 band origin. Therefore, the species **m1** can be assigned to conformer IV.

1.3 Comparison between B3LYP and M05-2X results

As described above, both the B3LYP and M05-2X results reproduce the observed IR spectra and electronic energies very well. However, the relative energies of the conformers are different between the two levels. Especially, boat conformer (III) has very high energy in M05-2X calculation; it is 1902 cm^{-1} higher than the most stable conformer II [Fig. 2(a)]. The reason of the high energy of the boat conformer at M05-2X calculation may be attributed that the M05-2X calculation properly takes into accounts of the CH···O and vdW interactions for the stabilization energies. In the structures of the conformers in Fig. 2, the crown frame of the conformers I, II, IV, and V is fixed by the CH···O or π···π interactions, while such interactions seem very weak in the boat conformer. This difference may lead the boat conformer to higher energy than others at M05-2X calculation. On the other hand, B3LYP seems not to properly take into account the CH···O and vdW interactions, and all the conformers have similar energies.

The M05-2X calculation explains why the boat conformer is not experimentally

observed in the jet; the energy of the boat conformer is too high to exist as a bare conformer. It is very interesting that the boat conformer becomes most stable in both calculations when it incorporates a water molecule in its cavity [Fig. 2(b)]. The reason why the boat conformer emerges upon the complexation with a H_2O molecule is that the stabilization by the H-bonding is remarkably larger than the weak CH···O and vdW interactions. In the next sections, we discuss structures of complexes based on only results of the M05-2X calculation since it reproduces well the relative energies of bare conformers.

2. DB18C6 complexes with ammonia, methanol, and acetylene

2-1. Electronic spectra

Fig. 4 shows the LIF spectra of (a) bare DB18C6 and DB18C6-H_2O, (b) DB18C6-ammonia, (c) DB18C6-methanol, and (d) DB18C6-acetylene complexes. In the LIF spectrum of the complex with ammonia [Fig. 4(b)], many sharp bands appear in the wide energy region. On the other hand, only a few bands appear in the LIF spectra of the complexes with methanol and acetylene [Fig. 4(c), (d)]. A further increase of the partial pressure of methanol or acetylene resulted in only an increase of broad background fluorescence signal.. Fig. 4 also shows the UV-UV HB spectra obtained by monitoring the labeled bands in the LIF spectra. From the UV-UV HB spectroscopy, nine (A-I), one (J), and two (K, L) species can be identified for each complex.

Fig. 5 shows IR-UV DR spectra in the methylene CH stretching region of the complexes identified in the LIF spectra (Fig. 4). For comparison, the IR spectra of **m1**, **m2**, and **a** are also shown. We found that the species can be classified into two groups according to the IR spectral patterns; (a) the species showing IR spectra similar to those

of the species **m1** and **m2**, (b) the ones similar to that of the species **a**. The bands labeled by an asterisk in the spectrum of species **J** (DB18C6-methanol complex) are due to the CH stretching vibrations of the methyl group of CH_3OH[15]. The classification in Fig. 5 makes it clear that in the species **A, C, D, J, K,** and **L** [Fig. 5(a)], the DB18C6 conformations are very similar to either of **m1** or **m2** (bare conformers), while the species **B, E, F, G, H,** and **I** [Fig. 5(b)] have DB18C6 conformation similar to that of the species **a** (boat-H_2O). Therefore, the boat DB18C6 conformation may be also formed in the complexes **B, E, F, G, H,** and **I**. Very interestingly, the conformational change into the boat conformation occurs only for the complexation with ammonia, but not with methanol or acetylene. This implies that DB18C6 recognize the difference of the guest species upon the complexation.

From the analysis of the IR-UV DR spectra in the methylene CH stretching region, we find that the species **B, E, F, G, H,** and **I** have the boat conformation similar to the species **a** [Fig. 5(b)]. However, for the species **A, C, D, J, K,** and **L** [Fig. 5(a)], the DB18C6 conformation cannot be determined to which of **m1** or **m2**, simply for the IR spectra. To solve this problem, we compared UV-UV HB spectra of the species **A, C, D, J, K,** and **L** with those of the species **m1** and **m2**. Fig. 6 shows the UV-UV HB spectra of the species **m1**, **m2**, **A, C, D**, **J**, **K** and **L**. The energy of the horizontal axis is taken relative to each origin band. The UV-UV HB spectrum of **m1** [Fig. 6(a)] shows three prominent peaks in the 80-120 cm^{-1} region, while that of **m2** [Fig. 6(b)] shows rich vibrational structures in the lower frequency region, 10-80 cm^{-1}. By comparing the UV-UV HB spectra of the complexes with the two spectra, we can find the spectra of species **A** and **J** are similar to **m1** [Fig. 6(a)], and those of the species **C, D, K,** and **L** are similar to **m2** [Fig. 6(b)]. Therefore, it is concluded the DB18C6 conformations of

the species **A** and **J** to be the **m1** (conformer IV) type and those of species **C, D, K,** and **L** to the **m2** (conformer I) type. In Table 1, the positions of origin bands, type of complex, DB18C6 conformation, equivalency of environment between two chromophores, symmetry, and assignment are listed for all the species.

2.2 Structures of the complexes formed without conformational change

2.2.1 DB18C6-ammonia complexes

Here we discuss the structures of the DB18C6-ammonia complexes in which DB18C6 conformation is the same with that of the species **m1** or **m2**, that is, the species **A**, **C**, and **D**. Fig. 7(a) shows IR-UV DR spectra of these complexes in the region of the NH stretching vibrations. In the IR-UV DR spectra, the bands at 3316-3317 cm^{-1} are ν_1 and those at 3402-3422 cm^{-1} are ν_3 of ammonia. The ν_3 mode is a degenerated vibration in the gas phase NH_3, but split into two by H-bonding. The number of the bands indicates that the species **A**, **C**, and **D** are the DB18C6-NH_3 complex. The frequencies of these vibrations are red-shifted by ~20 cm^{-1} with respect to those of gas phase NH_3 (ν_1=3337, ν_3=3444 cm^{-1})[16]. This situation is similar to the oxindole-NH_3 complex (ν_1=3313, ν_3=3406, 3436 cm^{-1}) where NH_3 acts as a H-donor to an O atom of C=O as well as a H-acceptor of the amide NH group[17]. When NH_3 acts as only H-acceptor, ν_1 and ν_3 modes are not so red-shifted; phenol-NH_3 (ν_1 = 3333 cm^{-1})[18] and 2-naphthol-NH_3 (ν_1 = 3333, ν_3 = 3434 cm^{-1})[19], suggesting that the NH_3 molecule in the species **A**, **C**, and **D** is H-bonded to DB18C6 as H-donor. The ν_3 frequency of species **A** (3402 cm^{-1}) is lower than those of the species **C** and **D**, implying that the NH_3 molecule in the species A is more strongly H-bonded to DB18C6 than in the species **C** and **D**.

Figs. 8(a) and (b) show the five most stable optimized structures of DB18C6-NH_3

complexes obtained at M05-2X/6-31+G* level. The lower panel of Fig. 7(a) shows the calculated IR spectra of the DB18C6-NH_3 complexes. In the calculated IR spectra [Fig. 7(a)], the frequencies of the IR bands of IV-NH_3-1 complex are located in the lowest region among the five isomers of DB18C6-NH_3. In the observed IR spectra, the species **A** shows the lowest vibrational frequencies. So, the species **A** probably corresponds to the IV-NH_3-1 complex. In the IV-NH_3-1 structure [Fig. 8(a)], a NH_3 molecule fits into the cavity of the IV conformation and is H-bonded to the O_6 and O_2 atoms, forming bidentate H-bond. In addition, the methylene CH of the crown frame is H-bond to the N atom of NH_3. Such a good fit to the crown cavity causes the stronger H-bonds and results in the IV-NH_3-1 complex to be the most stable structure. For other isomers of DB18C6-NH_3, they do not show remarkable difference in the IR spectra, and the determination of the structures for the species **C** and **D** is difficult based on the comparison with calculated IR spectra.

So, for the additional information of the complex assignments, we calculated the electronic transition energies of the complexes by TDDFT. Fig. 9(a) shows the calculated transition energies of I-NH_3-*n* (*n* = 1, 2, 3) (black sticks), and those of IV-NH_3-*n* (*n* = 1, 2) (yellow sticks), which are compared with the LIF spectrum and the calculated transition energies of bare IV and I conformers (green sticks). We see the calculated band position of IV-NH_3-1 coincides with that of **A**, which is in good agreement with the assignment based on the IR spectra. As was described above, the complexes **C** and **D** have the conformation I (Table 1). Since the positions of calculated electronic transition energies of I-NH_3-1 and I-NH_3-3 (black sticks) correspond to bands **D** and **C,** respectively, the species **D** and **C** are assignable to the I-NH_3-1 and I-NH_3-3 complexes. The geometries, IR spectra, and S_1-S_0 transition energies of the other

isomers with the higher relative energies are shown in ESI.

2.2.2 DB18C6-methanol complexes

The IR-UV DR spectrum of the DB18C6-methanol complex (species **J**) in the OH stretching vibrational region is shown in the upper panel of Fig. 7(b). Since the spectrum shows only one band at 3518 cm^{-1}, species **J** is DB18C6-CH_3OH. The band at 3518 cm^{-1} is red-shifted by 164 cm^{-1} from the gas phase CH_3OH (3682 cm^{-1})[16]. This large red-shift indicates that the OH group of CH_3OH is H-bonded to ether oxygen because the OH band with O···π H-bonding appears at higher frequency: 3639 cm^{-1} in benzene-CH_3OH[15] and 3584 cm^{-1} in [dibenzo-24-crown-8(DB24C8)]-CH_3OH[7(e)].

Fig. 8(c) shows the three most stable optimized structures built on the IV conformation. The DB18C6 part of the species **J** was already determined to be the IV conformation (Table 1), so that the three isomers are probable structures for the species **J**. In IV-CH_3OH-1 complex, a CH_3OH molecule is fit into the cavity of the IV conformation: OH···O_6, CH···O_2, and methylene CH···OH, resulting in the lowest energy. So, IV-CH_3OH-1 isomer is assignable to the species **J**. The lower panel in Fig. 7(b) shows the calculated IR spectra of the optimized structures, and Fig. 9(b) shows the calculated S_1-S_0 transition energies of IV-CH_3OH-*n* (*n* = 1-3, yellow sticks). Though it is difficult to determine the structure of the species **J** from the position of the OH stretching band alone, the S_1-S_0 transition energy of the IV-CH_3OH-1 reproduce well that of the species **J**.

2.2.3 DB18C6-acetylene complex

Fig. 7(c) shows IR-UV DR spectra of DB18C6-acetylene complex in the region of

the CH stretching vibration of acetylene. A sharp band due to anti-symmetric CH stretching vibration (ν_3) of C_2H_2 appears at 3252 and 3242 cm^{-1} in the spectra of species **K** and **L**, respectively, so the species **K** and **L** are DB18C6-C_2H_2. The band positions are largely red-shifted from ν_3 of bare C_2H_2 (3289 cm^{-1}, which is the depertubed frequency from the Fermi resonance)[20]. In the C_2H_2-H_2O complex[21], the ν_3 mode of C_2H_2 which acts as H-donor to H_2O appears at 3240 cm^{-1}, while the ν_3 modes of C_2H_2 molecules which are H-bonded to the π-electrons appear in the 3256-3267 cm^{-1} region[20]. Thus, in the species **K,** C_2H_2 is probably H-bonded to the π-electrons, and in the species **L,** C_2H_2 is H-bonded to ether oxygen.

Fig. 8(d) shows the three most stable optimized structures of the DB18C6-C_2H_2 complexes constructed on the conformation I. Since the conformations of the DB18C6 part in the species **K** and **L** are the conformation I (Table 1), the optimized complexes are probable structures for the species **K** and **L**. The IV-C_2H_2-1 and IV-C_2H_2-2 isomers form the CH···π H-bonding, and IV-C_2H_2-3 forms the bifurcated CH···O H-bonding. Since IV-C_2H_2-2 is the transition state, species **K** can be assigned to IV-C_2H_2-1, and species **L** to IV-C_2H_2-3. The lower panel of Fig. 7(c) shows the calculated IR spectra of the optimized structures, and Fig. 9(c) shows the calculated S_1-S_0 transition energies of I-C_2H_2-*n* (*n* = 1-3, black sticks). The calculated IR spectra reproduce well the ν_3 positions of C_2H_2 H-bonded to π-electrons and the ether oxygen atom, and the S_1-S_0 transition energies of IV-C_2H_2-1 and IV-C_2H_2-3 also reproduce well those of the species **K** and **L**, respectively.

2.3 Structure of the DB18C6 complexes accompanied by conformational change

2.3.1 DB18C6-$(NH_3)_n$ (n=1-3)

Here we discuss the structures of the DB18C6-ammonia complexes in which DB18C6 has the boat conformation: the species **B, E, F, G, H,** and **I** (see Table 1). Fig. 10 shows IR-UV DR spectra of (a) the species **E, F,** (b) **B, G, H,** and (c) **I** in the region of NH stretching vibrations. The species **E** and **F** show similar spectral patterns with each other, where ν_1 (3314 cm^{-1}) and ν_3 (~3400 and 3418 cm^{-1}) of NH_3 are observed. The ν_3 frequencies (~3400, 3418 cm^{-1}) are close to those of the species **A** [3402, 3422 cm^{-1}, Fig. 7(a)], implying that in the species **E** and **F**, NH_3 is H-bonded in the bidentate manner similar to the species **A [**IV-NH_3-1, Fig. 8(a)]. For the species **B**, **G**, and **H,** they show similar spectral patterns with each other [Fig. 10(b)]. Comparing with IR-UV DR spectra of the species **E** and **F**, prominent peaks are seen at ~3200, ~3240, and ~3575 cm^{-1} in those of the species **B, G**, and **H**. The appearance of the bands at ~3200, ~3240 cm^{-1} indicates the presence of the NH···N hydrogen-bonding, suggesting the presence of $(NH_3)_2$ structure in the complexes. The reason why there are two bands in the region of the H-bonded NH stretching vibrations can be explained by Fermi resonance between H-bonded NH stretching vibration (ν_1) and bending overtone (2×1627.5 cm^{-1})[16-19, 22]. For example, the H-bonded NH stretching vibration of the ring-form 2-phenol-$(NH_3)_2$ complex[22(a)] appears at 3219 and 3239 cm^{-1}. In the Fig. 10(c), the species **I** shows IR bands of not only NH stretching vibrations (3316, 3407, and 3414 cm^{-1}) of NH_3 but also the OH stretching vibrations (3577 and 3650 cm^{-1}) of H_2O, indicating that the species **I** is boat-H_2O-NH_3 complex, so that the species **I** is discussed in the next section.

Fig. 10 also shows the most probable optimized structures assignable to the species **E, F, B, G,** and **H**. Their calculated IR spectra are shown at lower panel of each IR-UV spectrum. In the boat-NH_3-1 complex, the NH_3 molecule forms bifurcated and bidentate H-bond at the bottom of the boat conformation, similar to the boat-H_2O complex [Fig.

2(b)]. The IR spectra of boat-NH_3-1 shows a ν_1 band at 3260 cm^{-1}, and two ν_3 bands at 3362 and 3385 cm^{-1}. In boat-$(NH_3)_2$-1 complex, second NH_3 molecule forms another bidentate H-bonding at the top of the boat conformation. The IR spectra of boat-NH_3-1 and boat-$(NH_3)_2$-1 are very similar with each other except that the latter spectrum is slightly broadened due to the overlap of two bands. Both the calculated IR spectra of boat-NH_3-1 and boat-$(NH_3)_2$-1 well reproduce the observed IR bands of **E** and **F**, respectively. In the boat-$(NH_3)_2$-2, boat-$(NH_3)_2$-3, and boat-$(NH_3)_3$-1 complexes, $(NH_3)_2$ is located at the top or bottom of the boat DB18C6 and forms H-bond to ether oxygen atoms. In the boat-$(NH_3)_3$-1 complexes, third NH_3 is independently H-bonded to the boat conformation. All the complexes show bands at ~3180 cm^{-1} attributed to the ν_1 band of the H-donor in $(NH_3)_2$. In addition, ν_3 band is further red-shifted or split as shown in the calculated spectra of boat-$(NH_3)_2$-2, boat-$(NH_3)_2$-3 and boat-$(NH_3)_3$-1. The calculated spectra well reproduce the observed spectra, except the doublet structure at 3200-3240 cm^{-1} due to Fermi resonance. It should be noted that in the UV-UV HB spectra of the species **E** and **G** [Fig. 4(b)], their origins show ~5 cm^{-1} exciton splitting, similar to the species **m2** and **a**, suggesting that in the species **E** and **G**, the conformations of crown frame near the two chromophores is similar. Since the structures corresponding to the species **E** and **G** (boat-NH_3-1 and boat-$(NH_3)_2$-3, respectively) have equivalent chromophores, these assignments are reasonable. Furthermore, the calculated S_1-S_0 transition energies of all the optimized structures shown in Fig. 10 reproduce well the position of the observed ones [Fig. 9(a)].

2.3.2 DB18C6-H_2O-NH_3 complex

The IR-UV DR spectra of the species **I** [Fig. 10(c)] exhibits OH stretching

vibrations (3577 and 3650 cm^{-1}) as well as NH ones (3316, 3407 and 3414 cm^{-1}), so that the species **I** is boat-H_2O-NH_3. Since the bands of OH stretching vibrations in the species **a** (boat-H_2O)[7(b)] appear at 3580 and 3648 cm^{-1}, it is clear that the bands at 3577 and 3650 cm^{-1} are due to the bidentately H-bonded H_2O. The most probable optimized structure of the species **I** is shown at the right side of Fig. 10(c) (boat-H_2O-NH_3-1), and the calculated IR spectrum is shown at the lower panel of Fig. 10(c). In the boat-H_2O-NH_3-1 complex, both H_2O and NH_3 molecules are H-bonded in the bidentate way, and the calculated spectrum reproduces well the observed one. As shown in Fig. 9(a), the calculated S_1-S_0 transition energy of the boat-H_2O-NH_3-1 complex also agrees with the position of species **I**.

Conclusion

The conformation of dibenzo-18-crown-6 (DB18C6) and the structures of the DB18C6 (host) complexes with water, ammonia, methanol, and acetylene (guest) were investigated by laser induced fluorescence (LIF), UV-UV hole-burning (UV-UV HB), and IR-UV double-resonance (IR-UV DR) spectroscopy with the aid of density functional theory (DFT) calculations. The conformation of bare DB18C6 was reinvestigated by analyzing the IR-UV DR spectra of the methylene CH stretching vibrations. It is concluded that the "boat" conformation, which was previously assigned to the lowest energy conformer, does not exist as bare form under tthe jet-cooled condition. The boat conformer is found to be much unstable as bare conformer at the M05-2X/6-31+G* calculation. With the aid of Monte Carlo simulation for broad conformational search, the observed two conformers, **m1** and **m2,** are assigned to low energy conformers having C_1 and C_2 symmetry, respectively.

For the DB18C6-H_2O complex, its IR-UV DR spectrum of methylene CH stretching vibrations is considerably different from those of the bare conformers. From the analysis by DFT calculations, and we concluded that the DB18C6 conformation in the DB18C6-H_2O complex is the boat conformation. The structure of the DB18C6-H_2O complex is the same with one assigned in our previous paper based on the IR-UV DR spectrum in the region of OH stretching vibrations. The difference of the DB18C6 conformation between bare conformers and DB18C6-H_2O implies that DB18C6 changes its own conformation upon the complexation with H_2O.

For the DB18C6 complexes with ammonia, methanol, and acetylene, we identified nine, one, and two species, respectively, in each LIF spectrum. Among them, similar conformational change was observed in the DB18C6-ammonia complexes. On the other hand, in the complexes with methanol and acetylene, DB18C6 does not change its conformation and retains the same conformation with the bare form. By analyzing IR-UV DR spectra in the region of CH, NH, and OH stretching vibrations, all the complexes' structures were assigned. In the complexes with ammonia, a NH_3 molecule is incorporated into the cavity of the boat conformation through bidentate and bifurcated H-bonding, similar to DB18C6-H_2O. So, a key point for the conformational change is the incorporation in the boat conformation via bidentate H-bonding between DB18C6 and guest molecules. On the contrary, in the DB18C6-methanol and -acetylene complexes, CH_3OH and C_2H_2 molecules are simply bound to the oxygen atom or π-electrons of benzene rings. Therefore, we can say that DB18C6 recognizes the difference of the shape of guest species, and changes the conformation if guest species has an ability of bidentate H-bonding.

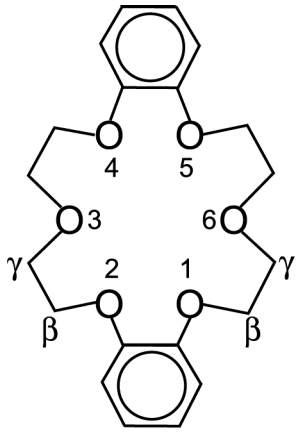

Scheme 1 DB18C6

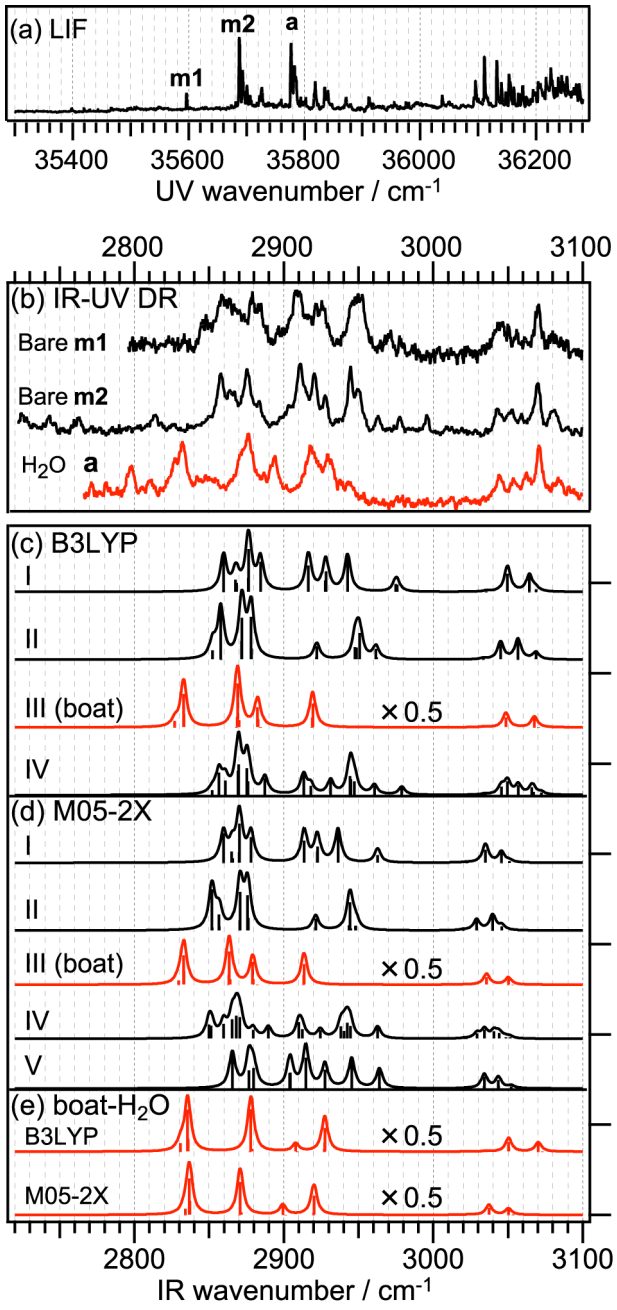

Fig. 1 (a): LIF spectrum of bare DB18C6 conformers (**m1** and **m2**) and DB18C6-H_2O (species **a**). (b): IR-UV DR spectra of **m1**, **m2**, and **a**. (c), (d): Calculated IR spectra of optimized conformers at B3LYP and M05-2X levels, respectively. (e): Calculated IR spectra of boat-H_2O obtained by B3LYP and M05-2X calculations. The optimized geometries are shown in Fig. 2. The intervals between the tips of the right axis represent 200 km/mol calculated IR intensity

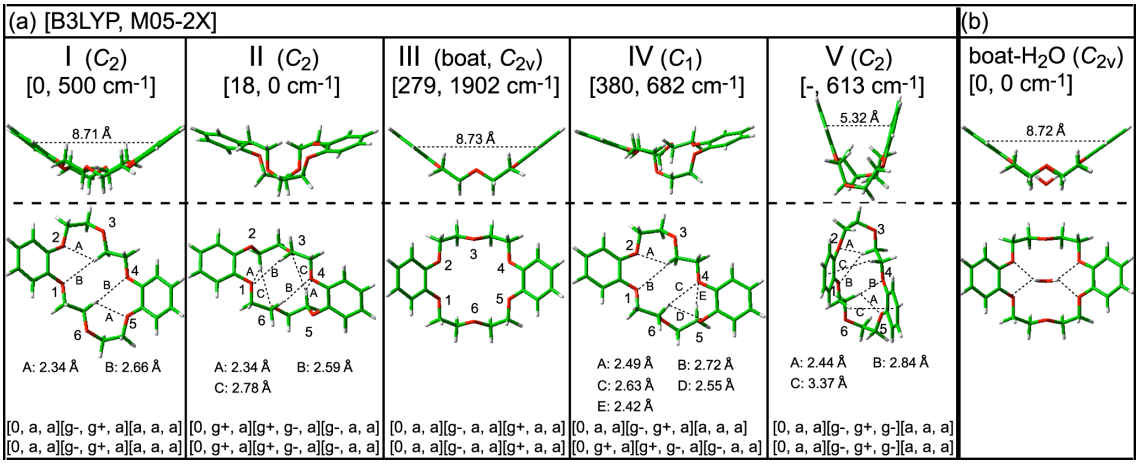

Fig. 2 Optimized geometries of (a) bare conformers and (b) DB18C6-H_2O. Except for conformer V, all the geometries are obtained by geometrical optimizations at B3LYP and M05-2X levels with 6-31+G* basis set. Relative energies with respect to the most stable conformer in the corresponding calculated levels are represented in cm^{-1} unit ([B3LYP, M05-2X]). The distances of CH···O, CH···π, and π···π in optimized geometries at the M05-2X calculation are indicated in the figure. In the bottom of each column, conformations of dihedral angles of -O-C-C-O-, -C-C-O-C-, and -C-O-C-C- units in the crown ring are indicated in each parenthesis. For example, the first parenthesis: [-O_1-C=C-O_2-, -C-C-O_2-C-, -C-O_2-C-C-], the second parenthesis: [-O_2-C-C-O_3-, -C-C-O_3-C-, -C-O_3-C-C-], etc., where -C=C- means carbon atoms in benzene ring. The labels "0", "a", "g+", and "g–" represent dihedral angles of -O-C=C-O- (~0º), anti (~180º), gauche+ (~ +60º), and gauche- (~ –60º), respectively.

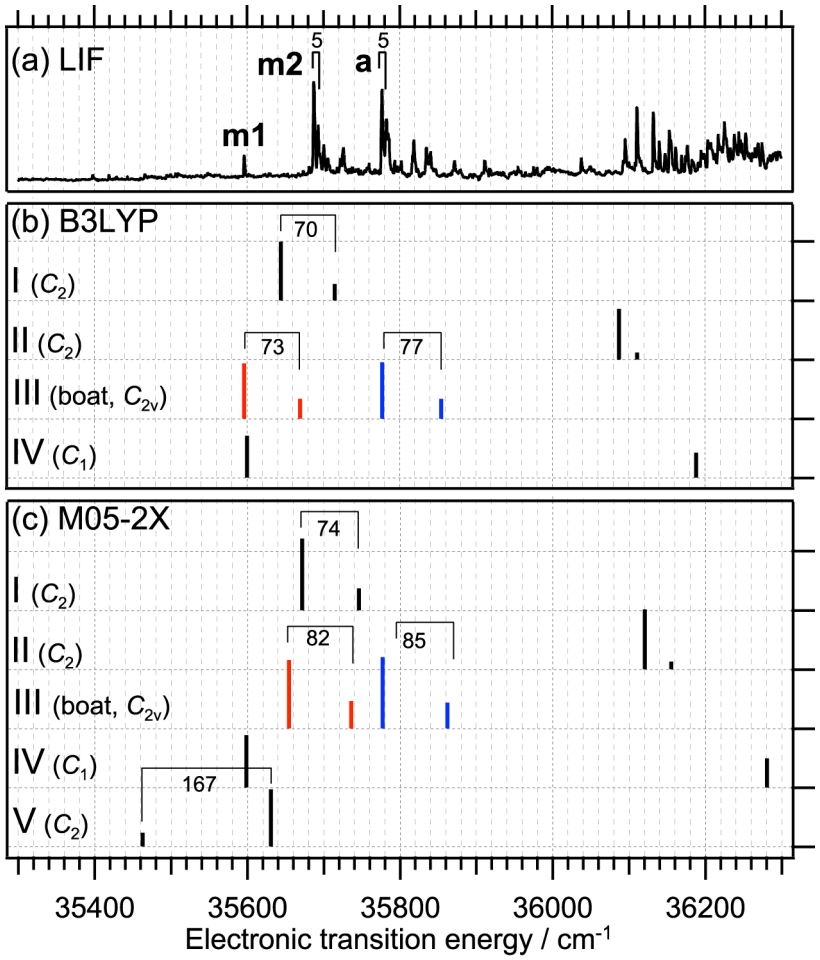

Fig. 3 (a): LIF spectrum of bare DB18C6 conformers and DB18C6-H_2O. (b), (c): S_1-S_0 and S_2-S_0 electronic transition energies obtained by TDDFT calculations at B3LYP and M05-2X levels, respectively, which are represented by red and black stick bars for bare conformers and by blue bars for boat-H_2O. The red and black colors correspond to the colors of calculated IR spectra in Fig. 1. The intervals between the tips of the right axis represent 0.1 oscillator strength.

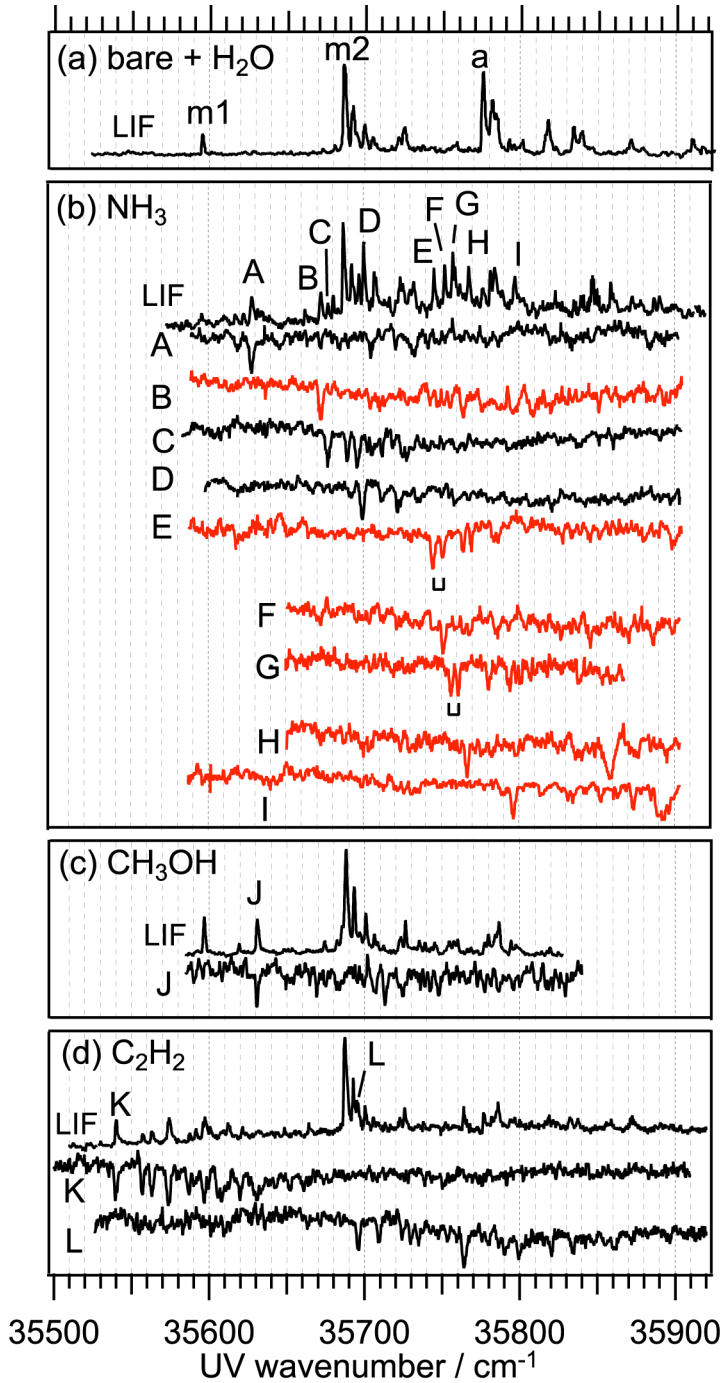

Fig. 4 (a): LIF spectrum of bare DB18C6 and DB18C6-H_2O. (b)-(c): LIF and UV-UV HB spectra of the complexes with ammonia, methanol, and acetylene, respectively.

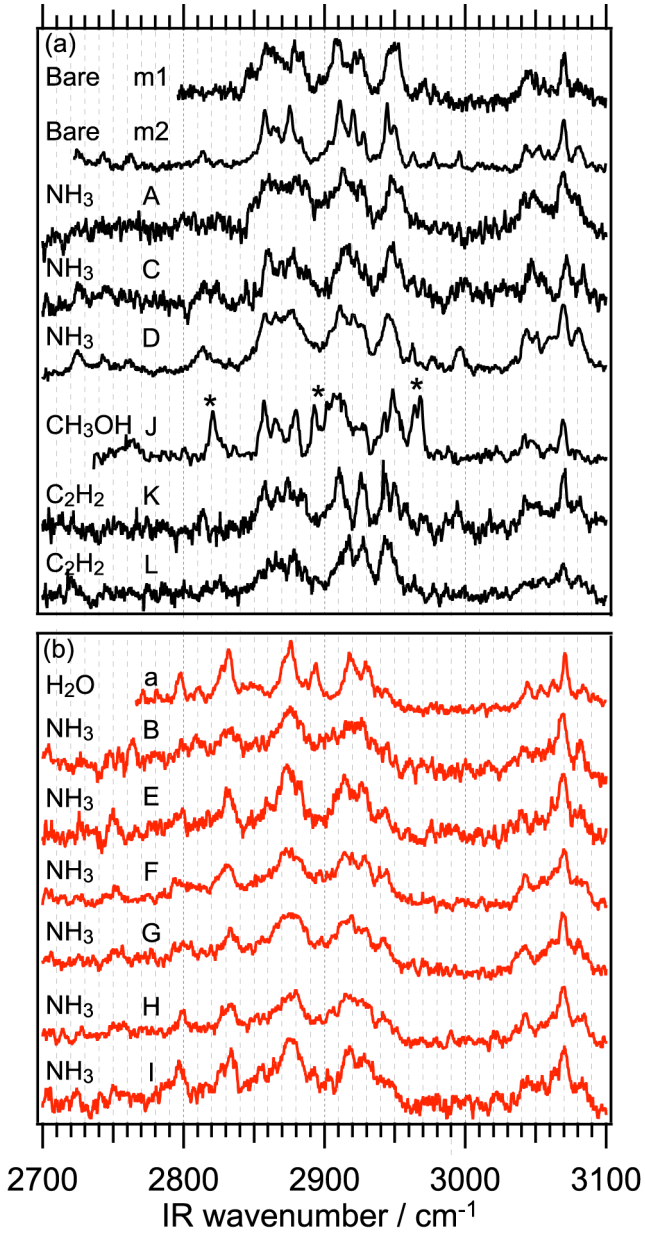

Fig. 5 IR-UV DR spectra in the region of CH stretching vibrations of the complexes with ammonia (species A-I), methanol (species J), and acetylene (species K and L). These IR spectra are classified into two groups: (a) IR spectral patterns similar to those of species **m1** and **m2,** (b) ones similar to that of species **a**. The IR-UV DR spectra of bare conformers (species **m1** and **m2**) and DB18C6-H_2O (species **a**) are also shown for comparison.

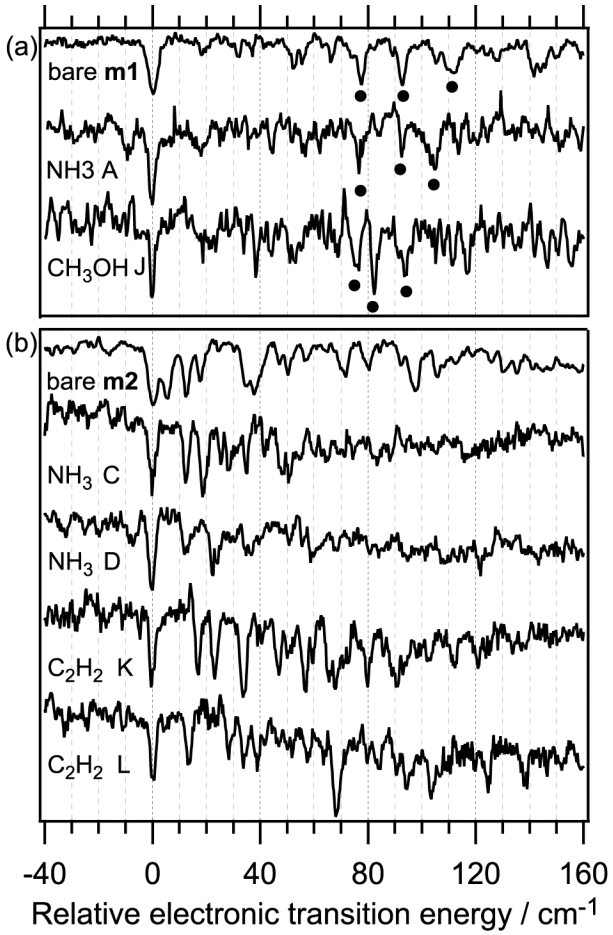

Fig. 6 UV-UV HB spectra of species **m1**, **m2** (bare), A, C, D (DB18C6-NH_3), J (DB18C6-CH_3OH), K, and L (DB18C6-C_2H_2), plotted as a function of relative electronic transition energy with respect to each origin transition. These UV-UV HB spectra are classified into two groups: (a) vibronic spectral patterns similar to that of species m1, (b) those similar to that of species m2. All the species in this figure show methylene CH stretching vibrations similar to each other (Fig. 5).

Table 1 Position of origin bands, type of complex, DB18C6 conformation, equivalency between two chromophores, symmetry, and assignment.

species	origin / cm^{-1}	type of complex	DB18C6 conformation	equivalency of environment between two chromophores[a]	symmetry	assignment[b]
m1	35597	DB18C6	IV	inequivalent	C_1	
m2	35688	DB18C6	I	equivalent	C_2	
a	35777	DB18C6-H_2O	III (boat)	equivalent	C_{2v}	
A	35628	DB18C6-NH_3	IV	inequivalent	C_1	1
B	35673	DB18C6-$(NH_3)_2$	III (boat)	inequivalent	C_1	2
C	35677	DB18C6-NH_3	I	inequivalent	C_1	3
D	35700	DB18C6-NH_3	I	inequivalent	C_1	1
E	35745	DB18C6-NH_3	III (boat)	equivalent	C_s	1
F	35752	DB18C6-$(NH_3)_2$	III (boat)	inequivalent	C_s	1
G	35757	DB18C6-$(NH_3)_2$	III (boat)	equivalent	C_s	3
H	35768	DB18C6-$(NH_3)_3$	III (boat)	inequivalent	C_1	1
I	35797	DB18C6-H_2O- NH_3	III (boat)	inequivalent	C_s	1
J	35631	DB18C6-CH_3OH	IV	inequivalent	C_1	1
K	35540	DB18C6-C_2H_2	I	inequivalent	C_1	1
L	35695	DB18C6-C_2H_2	I	inequivalent	C_1	3

[a] If equivalent, the species can show electronic exciton splitting (~5 cm^{-1})

[b] The end of digits in the labels of isomers (Fig. 8 and Fig. 10). For example, "3" of the species C represents the I-NH_3-3 isomer.

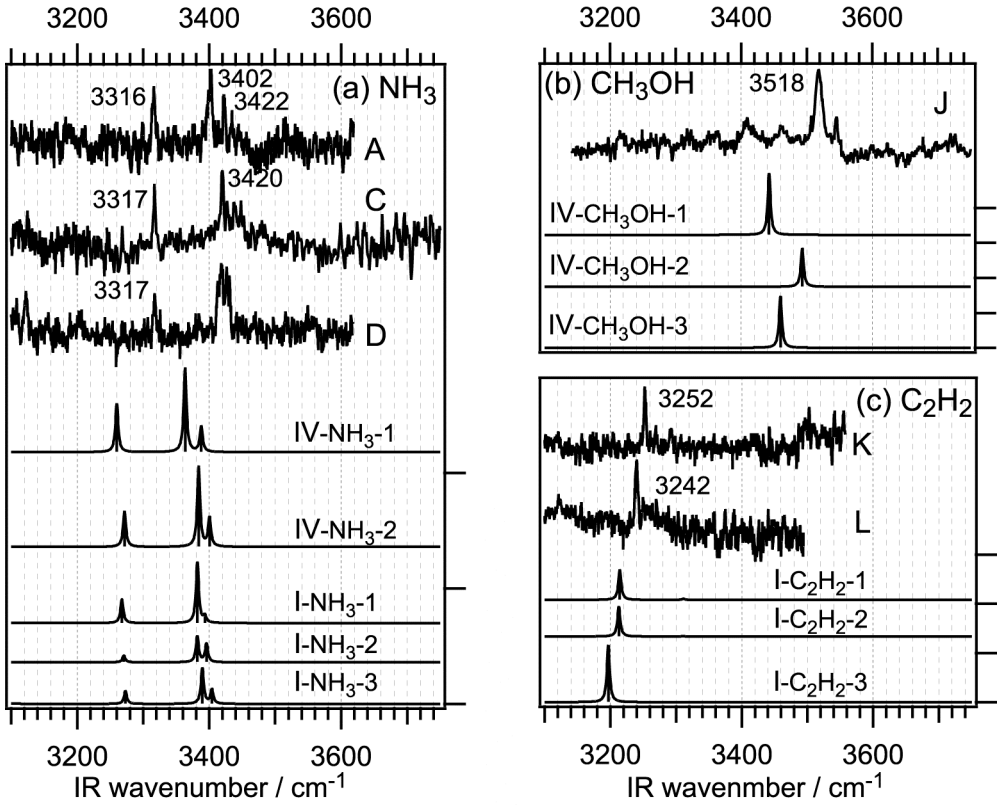

Fig. 7 IR-UV DR spectra of the complexes with (a) ammonia (species **A**, **C**, and **D**), (b) CH_3OH (species **J**), and (c) C_2H_2 (species **K** and **L**) in the region of NH, OH, and acetylene CH stretching vibrations, respectively. The lowers of each IR-UV DR spectrum are the calculated (M05-2X/6-31+G*) IR spectra of the optimized geometries in Fig. 8. The intervals between the tips in each right axis represent (a) 100, (b) 200, and (c) 200 kJ/mol calculated IR intensities. The calculated IR spectra are reproduced by providing the Lorentzian components with 5 cm^{-1} FWHM for each band.

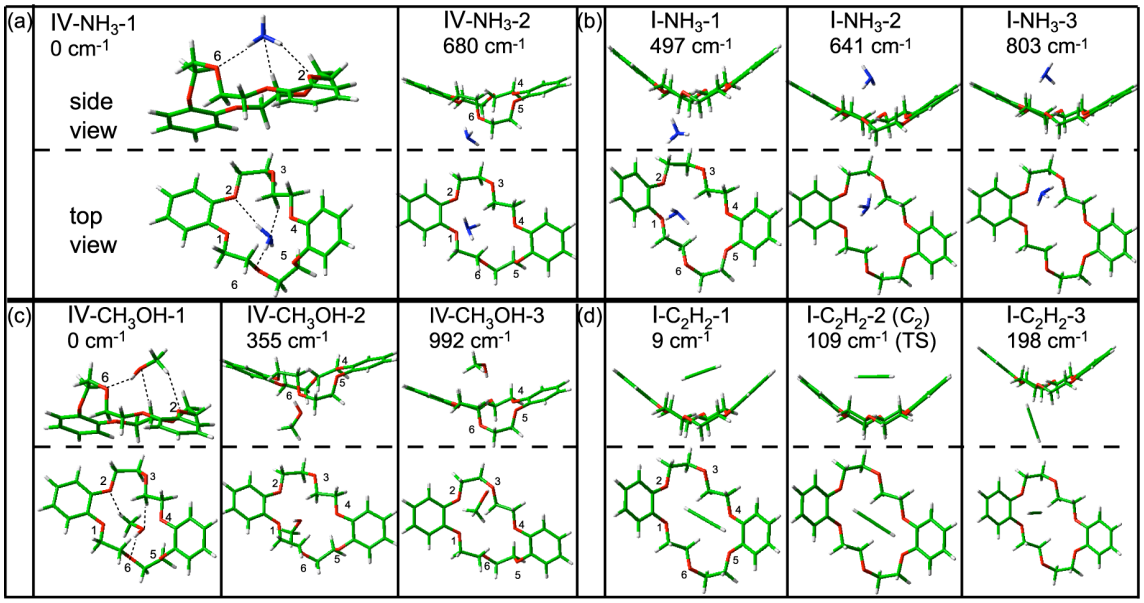

Fig. 8 Optimized geometries of (a) IV-NH_3, (b) I-NH_3, (c) IV-CH_3OH, and (d) I-C_2H_2 complexes obtained at the M05-2X/6-31+G* level. The geometries in (a) and (b) are the most five stable isomers in the obtained DB18C6-NH_3 complexes. The geometries in (c) and (d) are the most three stable isomers in IV-CH_3OH and I-C_2H_2 complexes, respectively.

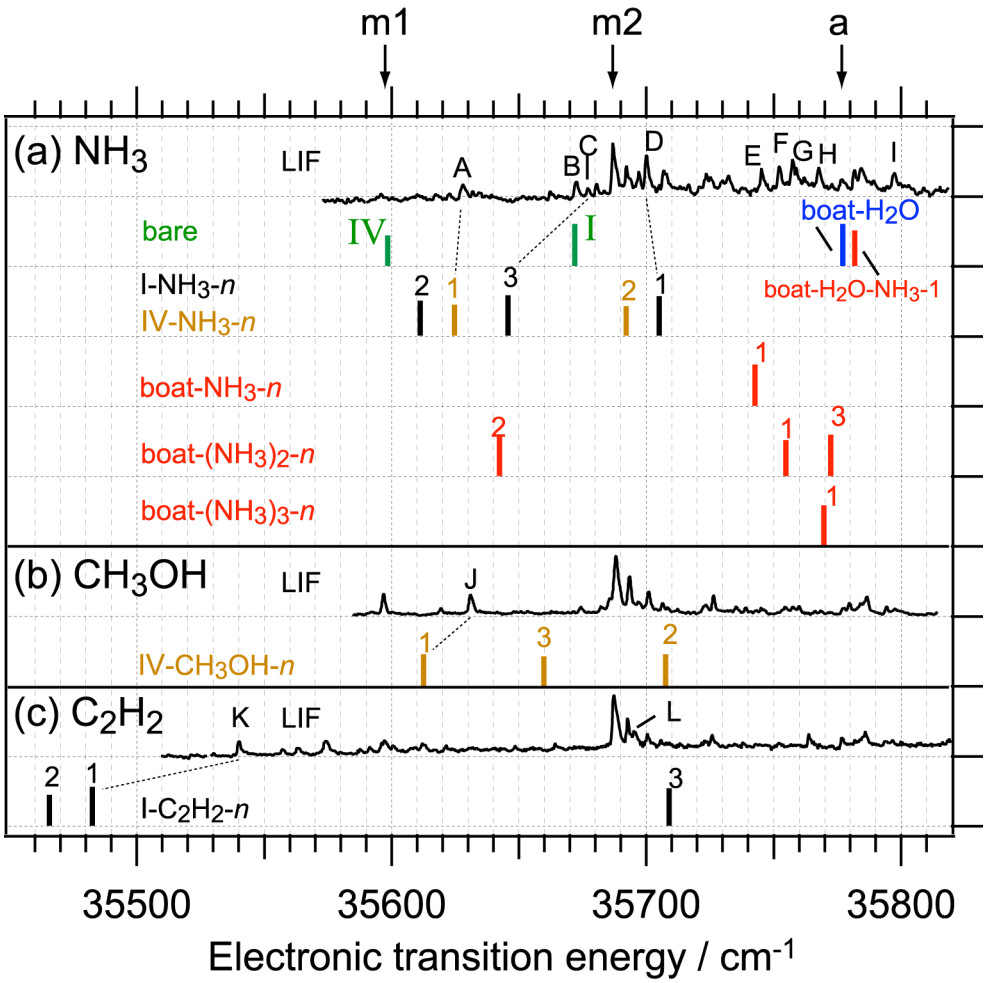

Fig. 9 S_1-S_0 electronic transition energies predicted by TDDFT (M05-2X/6-31+G*) calculations for DB18C6 complexes with (a) ammonia, (b) methanol, and (c) acetylene are shown as stick bars with each LIF spectrum. TDDFT results of bare conformers (conformers I and IV, green) and boat-H_2O (blue) are also shown for comparison. Black, yellow, and red colors indicate that DB18C6 conformations in the complexes are I, IV, and III (boat) conformations, respectively. Arabic numbers at the tops of the bars are used to identify a specific isomer among the isomers having the same DB18C6 conformation and the same number of the guest molecules in the same row. The intervals between the tips of the right axis represent 0.2 oscillator strength for the TDDFT results.

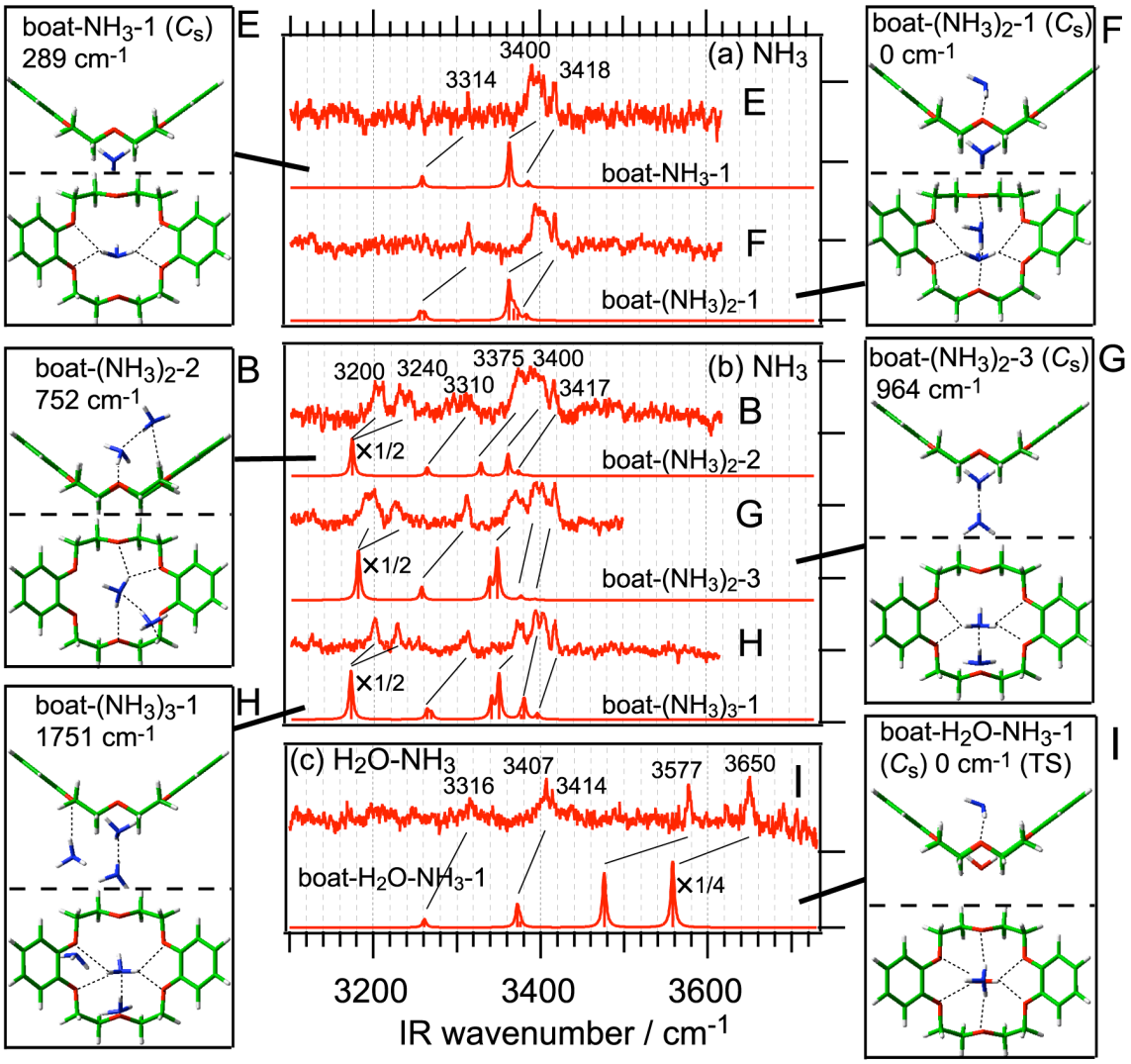

Fig. 10 IR-UV DR spectra of (a) species **E**, **F** (b) **B**, **G**, **H**, and (c) **I** in the region of NH and OH stretching vibrations. The calculated IR spectra (M05-2X/6-31+G*) of the most probable structures are shown under each IR-UV DR spectrum. The optimized geometries are also shown in this figure. Relative energies with respect to the most stable isomer are represented in cm^{-1} unit. The intervals between the tips in each right axis represent (a) 200, (b) 200, (c) 100 kJ/mol calculated IR intensities. The calculated IR spectra are reproduced by providing the Lorentzian components with 5 cm^{-1} FWHM for each band.

[1] (a) G. W. Gokel, *Crown Ethers and Cryptands*, Royal Society of Chemistry, Cambridge, UK, 1991. (b) M. Dobler, *Ionophores and their Structures*, Wiley-Interscience, New York, USA, 1981.

[2] (a) A. M. Stuart, J. A. Vidal, *J. Org. Chem.*, 2007, **72**, 3735. (b) N. Jose, S. Sengupta, J. K. Basu, *J. Mol. Catal. A: Chem.*, 2009, **309**, 153.

[3] (a) J. Malval, I. Gosse, J. Morand, R. Lapouyade, *J. Am. Chem. Soc.*, 2002, **124**, 904. (b) R. M. Uda, T. Matsui, M. Oue, K. Kimura, *J. Inclusion Phenom. Macrocyclic Chem.*, 2005, **51**, 111.

[4] (a) I. F. Uchegbu, S. P. Vyas, *Int. J. Pharm.*, 1998, **172**, 33. (b) L. Tavano, R. Muzzalupo, S. Trombino, I. Nicotera, C. O. Rossi, C. L. Mesa, *Colloids Surf., B*, 2008, **61**, 30.

[5] (a) R. M. Izatt, J. H. Rytting, D. P. Nelson, B. L. Hayamore, J. J. Christensen, *Science*, 1969, **164**, 443. (b) R. M. Izatt, D. P. Nelson, J. H. Rytting, J. J. Christensen, *J. Am. Chem. Soc.*, 1971, **93**, 1619. (c) C. J. Pedersen, H. K. Frensdorff, *Angew. Chem. Int. Ed.*, 1972, **11**, 16. (d) R. M. Izatt, R. E. Terry, B. L. Haymore, L. D. Hansen, N. K. Dalley, A. G. Avondet, J. J. Christensen, *J. Am. Chem. Soc.*, 1976, **98**, 7620. (e) R. M. Izatt, R. E. Terry, D. P. Nelson, Y. Chan, D. J. Eatough, J. S. Bradshaw, L. D. Hansen, J. J. Christensen, *J. Am. Chem. Soc.*, 1976, **98**, 7626. (f) J. D. Lamb, R. M. Izatt, C. S. Swain, J. J. Christensen, *J. Am. Chem. Soc.*, 1980, **102**, 475.

[6] (a) E. D. Glendening, D. Feller, M. A. Thompson, *J. Am. Chem. Soc.*, 1994, **116**, 10657. (b) D. M. Peiris, Y. Yang, R. Ramanathan, K. R. Williams, C. Watson, J. R. Eyler, *Int. J. Mass Spectrom. Ion Process.*, 1996, **157/158**, 365. (c) J. D. Anderson, E. S. Paulsen, D. Dearden, *Int. J. Mass Spectrom.*, 1999, **193**, 227. (d) M. B. More, D. Ray, P. D. Armentrout, *J. Am. Chem. Soc.*, 1999, **121**, 417. (e) S. E. Hill, D. Feller, *Int. J. Mass Spectrom.*, 2000, **201**, 41.

[7] (a) R. Kusaka, Y. Inokuchi, T. Ebata, *Phys. Chem. Chem. Phys.*, 2007, **9**, 4452. (b) R. Kusaka, Y. Inokuchi, T. Ebata, *Phys. Chem. Chem. Phys.*, 2008, **10**, 6238. (c) R. Kusaka, Y. Inokuchi, T. Ebata, *Phys. Chem. Chem. Phys.*, 2009, **11**, 9132. (d) R. Kusaka, Y. Inokuchi, S. S. Xantheas, T. Ebata, *Sensors*, 2010, **10**, 3519. (e) S. Kokubu, R. Kusaka, Y. Inokuchi, T. Haino, T. Ebata, *Phys. Chem. Chem. Phys.*, 2010, **12**, 3559.

[8] (a) V. A. Shubert, W. H. James III, T. S. Zwier, *J. Phys. Chem. A*, 2009, **113**, 8055. (b) V. A. Shubert, C. W. Müller, T. S. Twier, *J. Phys. Chem. A*, 2009, **113**, 8067.

[9] (a) T. Ebata, T. Hashimoto, T. Ito, Y. Inokuchi, F. Altunsu, B. Brutschy, P. Tarakeshwar, *Phys. Chem. Chem. Phys.*, 2006, **8**, 4783. (b) Y. Inokuchi, Y. Kobayashi, T. Ito, T. Ebata, *J. Phys. Chem. A*, 2007, **111**, 3209.

[10] I, Kolossváry, W. C. Guida, *J. Am. Chem. Soc.*, 1996, **118**, 5011.

[11] MacroModel, version 9.1, Schrödinger, LLC, New York, NY, 2005.

[12] T. A. Halgren, *J. Comput. Chem.*, 1999, 20, 730.

[13] M. J. Frisch, G. W. Trucks, H. B. Schlegel, G. E. Scuseria, M. A. Robb, J. R. Cheeseman, G. Scalmani, V. Barone, B. Mennucci, G. A. Petersson, H. Nakatsuji, M. Caricato, X. Li, H. P. Hratchian, A. F. Izmaylov, J. Bloino, G. Zheng, J. L. Sonnenberg, M. Hada, M. Ehara, K.

Toyota, R. Fukuda, J. Hasegawa, M. Ishida, T. Nakajima, Y. Honda, O. Kitao, H. Nakai, T. Vreven, J. A. Montgomery, Jr., J. E. Peralta, F. Ogliaro, M. Bearpark, J. J. Heyd, E. Brothers, K. N. Kudin, V. N. Staroverov, R. Kobayashi, J. Normand, K. Raghavachari, A. Rendell, J. C. Burant, S. S. Iyengar, J. Tomasi, M. Cossi, N. Rega, J. M. Millam, M. Klene, J. E. Knox, J. B. Cross, V. Bakken, C. Adamo, J. Jaramillo, R. Gomperts, R. E. Stratmann, O. Yazyev, A. J. Austin, R. Cammi, C. Pomelli, J. W. Ochterski, R. L. Martin, K. Morokuma, V. G. Zakrzewski, G. A. Voth, P. Salvador, J. J. Dannenberg, S. Dapprich, A. D. Daniels, O. Farkas, J. B. Foresman, J. V. Ortiz, J. Cioslowski, and D. J. Fox, Gaussian 09, Revision A.02, Gaussian, Inc., Wallingford CT, 2009.

[14] (a) Y. Zhao, D. G. Truhlar, *J. Phys. Chem. A,* 2006, **110**, 5121. (b) Y. Zhao, D. G. Truhlar, *Acc. Chem. Res.*, 2008, **41**, 157. (c) M. Prakash, K. G. Samy, V. Subramanian, *J. Phys. Chem. A*, 2009, **113**, 13845. (d) K. Y. Baek, M. Hayashi, Y. Fujimura, S. H. Lin, S. K. Kim, *J. Phys. Chem. A*, 2010, **114**, 7583.

[15] (a) R. N. Pribble, F. C. Hagemeister, T. S. Zwier, *J. Chem. Phys.*, 1997, **106**, 2145. (b) C. J. Gruenloh, G. M. Florio, J. R. Carney, F. C. Hagemeister, T. S. Zwier, *J. Phys. Chem. A.*, 1999, **103**, 496. (c) C. J. Gruenloh, G. M. Florio, J. R. Carney, F. C. Hagemeister, T. S. Zwier, *J. Phys. Chem. A.*, 1999, **103**, 503.

[16] G. Herzbeg, *Molecular Spectra and Molecular Structure Volume II. Infrared and Raman Spectra of Polyatomic Molecules*, Krieger, Malabar, USA, 1991.

[17] A. V. Fedorov, J. R. Cable, J. R. Carney, T. S. Zwier, *J. Phys. Chem. A*, 2001, **105**, 8162.

[18] A. Iwasaki, A. Fujii, T. Watanabe, T. Ebata, N. Mikami, *J. Phys. Chem.*, 1996, **100**, 16053.

[19] Y. Matsumoto, T. Ebata, N. Mikami, *J. Mol. Struct.*, 2000, **552**, 257.

[20] A. Fujii, S. Morita, M. Miyazaki, T. Ebata, N. Mikami, *J. Phys. Chem. A*, 2004, **108**, 2652.

[21] A. Engdahl, R. Nelander, *Chem. Phys. Lett*, 1983, **100**, 129.

[22] (a) S. Ishiuchi, K. Daigoku, M. Saeki, M. Sakai, K. Hashimoto, M. Fujii, *J. Chem. Phys.*, 2002, **117**, 7083. (b) Y. Matsuda, M. Mori, M. Hachiya, A. Fujii, N. Mikami, *Chem. Phys. Lett.*, 2006, **422**, 378.